

Families of meshes minimizing P_1 interpolation error for functions with indefinite Hessian

A. AGOUZAL*, K. LIPNIKOV†, and Yu. VASSILEVSKI‡

Abstract — For a given function, we consider the problem of minimizing the P_1 interpolation error on a set of triangulations with a fixed number of triangles. The minimization problem is reformulated as the problem of generating a mesh which is quasi-uniform in a specially designed metric. For functions with indefinite Hessian, we show the existence of a set of metrics with highly diverse properties. This set may include both anisotropic and isotropic metrics, which produce families of different meshes providing a comparable reduction of interpolation error. The developed theory is verified with numerical examples.

Let Ω_h be a conformal triangulation of a computational domain Ω and $\mathcal{S}_1(u)$ be a continuous piecewise linear Lagrange interpolant of a given function u . The interpolation error

$$e_h = u - \mathcal{S}_1(u)$$

depends on the triangulation. We consider the problem of minimizing this error on a set of triangulations with a fixed number of triangles. Methods developed for the solution of this problem can be used to decrease significantly the discretization error in various applications, including complex fluid flows [12]. A theoretical basis for this phenomenon exploits the fact that a discretization error can be bounded by the best interpolation error [9].

In many cases an approximate solution to this minimization problem is sufficient. In [18], we have shown that there exists a sequence of meshes that provide an asymptotically optimal reduction of the interpolation error in the $L^\infty(\Omega)$ -norm. These meshes were called quasi-optimal. The theory of quasi-optimal meshes has been extended to the $L^p(\Omega)$ -norm in [2, 19] and to the $W_2^p(\Omega)$ -norm in [2, 3]. In this paper we focus on the $L^\infty(\Omega)$ -norm of the interpolation error, although an extension of our main result to the $L^p(\Omega)$ -norm is possible.

A constructive approach to generating a quasi-optimal mesh is based on reformulating the minimization problem as a problem of building a mesh which is

*Université Lyon1, Laboratoire d'Analyse Numérique, Bat.101, 69 622 Villeurbanne Cedex, France

†Los Alamos National Laboratory, Los Alamos, NM 87545, U.S.A.

‡Institute of Numerical Mathematics, Moscow 119333, Russia. E-mail: vasilevs@dodo.inm.ras.ru

This research was partly supported by the Russian Foundation for Basic Research (grant 11-01-00971), the RAS program 'Optimal methods for problems of mathematical physics' and the Federal program 'Scientific and pedagogical staff of innovative Russia'.

quasi-uniform in a metric field. The metric-based mesh generation has a long and successful history (see e.g., [5–7, 10, 12, 13, 17] and references therein). Many methods have been developed using the common idea that the mesh size should be small in the regions of a strong solution gradient. A scalar metric proportional to the norm of the solution gradient is often called a monitor function [15]. It allows one to generate adaptive regular meshes for problems with isotropic solution singularities. A tensor metric derived from the Hessian of a solution is considered one of the best metrics nowadays [1, 7, 16–18]. It allows one not only to generate an adaptive mesh, but also to stretch it in the direction where the gradient is small.

To the best of our knowledge, the first theoretical justification that a Hessian-based metric results in an approximate solution of the minimization problem has been done in [1, 18]. An upper and a lower bounds have been derived there for functions with indefinite but nonsingular Hessians. Independently, a similar upper bound has been proved later in [8] for functions with definite Hessians. Upper bounds for P_k interpolation errors where $k > 1$ were proved in [16].

In [7, 13, 18] and similar papers, a Hessian is recovered from a discrete solution. The major theoretical disadvantage of this approach is that the recovered Hessian does not converge to the continuous one in the maximum norm on a sequence of refined meshes. An alternative technology has been proposed in [2–4]. There a metric is recovered from *a posteriori* error estimates prescribed to the mesh edges. Both approaches allow one to implement an automatic (black-box) mesh adaptation. The primary goal of the first approach is to minimize the interpolation error. The second one tackles the discretization error and is potentially more beneficial in problems where the discretization and interpolation errors differ significantly.

This paper extends the theory of quasi-optimal meshes to the P_1 interpolation problem. The main focus is on the functions with indefinite Hessian. In this case the existing theory leads to a single metric based on the spectral module of the Hessian, and hence to only one type of quasi-optimal meshes. Our new result is the existence of families of metrics with highly diverse properties. One metric can be isotropic, while another can be highly anisotropic. The developed theory explains why meshes quasi-uniform in different metrics still result in the optimal reduction of the interpolation error. The presented numerical examples show the sequences of quasi-optimal isotropic and anisotropic meshes where the interpolation errors differ within 1–3% across the sequences.

The paper outline is as follows. In Section 2 we develop the theory of multiple metrics that result in quasi-optimal meshes. In Section 3 we verify the theoretical findings with numerical examples. Concluding remarks are collected in Section 4.

1. Analysis of the P_1 interpolation error

To analyze the interpolation error, $e_h = u - \mathcal{I}_1(u)$, we employ the ‘divide and conquer’ approach. First, we prove error bounds for quadratic functions. Then we extend them to $C^2(\Omega)$ functions.

1.1. Bounds for quadratic functions

Let $\Omega \subset \mathfrak{R}^2$ be a bounded polygonal domain and Ω_h be its triangulation with $N(\Omega_h)$ triangles. Let $\mathcal{S}_1(u)$ be the continuous piecewise linear Lagrange interpolant of a given function u on the mesh Ω_h and $\mathcal{S}_{1,\Delta}(u)$ be its restriction to triangle Δ .

Let us consider a triangle Δ with vertices \mathbf{v}_i , $i = 1, 2, 3$, edge vectors $\mathbf{e}_k = \mathbf{v}_i - \mathbf{v}_j$, $k = 6 - i - j$, $1 \leq i < j \leq 3$. Let φ_i , $i = 1, 2, 3$, be linear functions on Δ associated with vertices \mathbf{v}_i , and $b_k = \varphi_i \varphi_j$ be quadratic bubble functions associated with edges \mathbf{e}_k . We define φ_i by requiring that $\varphi_i(\mathbf{v}_i) = 1$ and $\varphi_i(\mathbf{v}_j) = 0$ for $j \neq i$. Note that $0 \leq \varphi_i \leq 1$ and $0 \leq b_k \leq 1/4$ inside the triangle Δ .

We start analysis of the interpolation error for a quadratic function u_2 . The Hessian \mathbb{H}_2 of this function is constant. Since the local interpolation error $e_2 = u_2 - \mathcal{S}_{1,\Delta}(u_2)$ is zero at the vertices of the triangle Δ , we obtain easily the following Taylor formula:

$$e_2(\mathbf{x}) = -\frac{1}{2} \sum_{k=1}^3 (\mathbb{H}_2 \mathbf{e}_k, \mathbf{e}_k) b_k(\mathbf{x}).$$

Thus, we have

$$\|e_2\|_{L^\infty(\Delta)} \leq \frac{1}{8} \sum_{k=1}^3 |(\mathbb{H}_2 \mathbf{e}_k, \mathbf{e}_k)|. \quad (1.1)$$

The Hessian \mathbb{H}_2 is a symmetric matrix; therefore there exists a decomposition

$$\mathbb{H}_2 = \pm \mathbb{V}^T \mathbb{D} \mathbb{V} \quad (1.2)$$

where

$$\mathbb{D} = \begin{bmatrix} 1 & 0 \\ 0 & s \end{bmatrix}, \quad s = \text{sgn}(\det(\mathbb{H}_2)).$$

In the sequel, it is sufficient to assume that the Hessian is either positive definite, or indefinite; thus, we can consider only the plus sign in (1.2). The conclusions made for a positive definite Hessian will hold true for a negative one. The spectral module of \mathbb{H}_2 is defined as follows

$$|\mathbb{H}_2| = \mathbb{V}^T \mathbb{V}. \quad (1.3)$$

If $s = 1$, we obtain immediately that $\mathbb{H}_2 = |\mathbb{H}_2|$. Since $|\mathbb{H}_2|$ is positive definite, we can define a local metric as $\mathfrak{M}_\Delta = |\mathbb{H}_2|$. This approach has been extensively analyzed in the literature. It can be extended to general functions by approximating them locally as quadratic functions. The resulting piecewise constant metric \mathfrak{M} allows one to generate a quasi-optimal mesh. In this paper we look more closely at the case $s = -1$ where the Hessian is indefinite. We will show that, in addition to (1.3), there exist other metrics that produce quasi-optimal meshes with drastically different properties.

In the approach developed in [2, 18, 19], the maximum norm of e_2 is bounded from above by geometric quantities such as the length of the edges \mathbf{e}_k in metric $|\mathbb{H}_2|$:

$$\sum_{k=1}^3 |(\mathbb{H}_2 \mathbf{e}_k, \mathbf{e}_k)| \leq \sum_{k=1}^3 (|\mathbb{H}_2| \mathbf{e}_k, \mathbf{e}_k) = \sum_{k=1}^3 (\mathbb{V}^T \mathbb{V} \mathbf{e}_k, \mathbf{e}_k). \quad (1.4)$$

In the case $s = 1$, the above inequality becomes an identity. Here we try to improve the upper bound when $s = -1$ by exploiting the fact that the decomposition $\mathbb{H}_2 = \mathbb{V}^T \mathbb{D} \mathbb{V}$ is not unique. This results in the constrained minimization problem with respect to \mathbb{V} : Find $\mathfrak{M}_O = \mathbb{V}_o^T \mathbb{V}_o$ such that

$$\sum_{k=1}^3 |(\mathbb{H}_2 \mathbf{e}_k, \mathbf{e}_k)| \leq \sum_{k=1}^3 (\mathbb{V}_o^T \mathbb{V}_o \mathbf{e}_k, \mathbf{e}_k) = \inf_{\tilde{\mathbb{V}}: \tilde{\mathbb{V}}^T \mathbb{D} \tilde{\mathbb{V}} = \mathbb{H}_2} \sum_{k=1}^3 (\tilde{\mathbb{V}}^T \tilde{\mathbb{V}} \mathbf{e}_k, \mathbf{e}_k). \quad (1.5)$$

At this moment, we need to introduce an additional notation and prove a technical result. Let $[a | b]$ denote a 2×2 matrix with columns $a, b \in \mathfrak{R}^2$ and

$$\mathbb{Q} = \begin{bmatrix} 0 & -s \\ 1 & 0 \end{bmatrix}.$$

Lemma 1.1. *Let $\mathbb{H}_2 = \mathbb{V}^T \mathbb{D} \mathbb{V}$ and $\mathbb{H}_2 = \tilde{\mathbb{V}}^T \mathbb{D} \tilde{\mathbb{V}}$. Then, there exists a nonsingular matrix $\Phi = [\varphi | \varphi']$ such that $\tilde{\mathbb{V}} = \Phi \mathbb{V}$. Moreover, the vector $\varphi \in \mathfrak{R}^2$ satisfies $(\mathbb{D} \varphi, \varphi) = 1$ and $\varphi' = \mathbb{Q} \varphi$.*

Proof. The two decompositions imply that $\tilde{\mathbb{V}} = \Phi \mathbb{V}$ and $\Phi^T \mathbb{D} \Phi = \mathbb{D}$, which in turn implies that $(\det(\Phi))^2 = 1$. Thus, Φ is nonsingular. Moreover, $(\mathbb{D} \varphi, \varphi) = 1$, $(\mathbb{D} \varphi', \varphi') = s$ and $(\mathbb{D} \varphi, \varphi') = 0$. A direct verification shows that $\varphi' = \mathbb{Q} \varphi$ gives the last two identities. This proves the assertion of the lemma.

An immediate corollary of this lemma is that the local metric defined by (1.3) is unique when \mathbb{H}_2 is a positive definite matrix. Indeed, since $s = 1$, we have $(\varphi, \varphi') = 0$, which implies that Φ is an orthogonal matrix and

$$\tilde{\mathbb{V}}^T \tilde{\mathbb{V}} = \mathbb{V}^T \mathbb{V} = |\mathbb{H}_2| = \mathbb{H}_2.$$

Theorem 1.1. *Let Δ be a triangle with edges \mathbf{e}_k . Furthermore, let \mathbb{H}_2 be an indefinite matrix and $\mathbb{H}_2 = \mathbb{V}^T \mathbb{D} \mathbb{V}$ be one of the decompositions. Then, the solution to the minimization problem (1.5) is*

$$\mathfrak{M}_O \equiv \mathbb{V}_o^T \mathbb{V}_o = \frac{1}{\sqrt{\mu^2 - \lambda^2}} \mathbb{V}^T \begin{bmatrix} \mu & -\lambda \\ -\lambda & \mu \end{bmatrix} \mathbb{V} \quad (1.6)$$

where

$$\mu = \sum_{k=1}^3 (\mathbb{V} \mathbf{e}_k, \mathbb{V} \mathbf{e}_k), \quad \lambda = \sum_{k=1}^3 (\mathbb{R} \mathbb{V} \mathbf{e}_k, \mathbb{V} \mathbf{e}_k) \quad (1.7)$$

and

$$\mathbb{R} = \begin{bmatrix} 0 & 1 \\ 1 & 0 \end{bmatrix}.$$

Proof. Using Lemma 1.1, we obtain the following representation of the matrix $\tilde{\mathbb{V}}^T \tilde{\mathbb{V}}$:

$$\tilde{\mathbb{V}}^T \tilde{\mathbb{V}} = \mathbb{V}^T [\boldsymbol{\varphi} | \boldsymbol{\varphi}']^T [\boldsymbol{\varphi} | \boldsymbol{\varphi}'] \mathbb{V} = \|\boldsymbol{\varphi}\|^2 \mathbb{V}^T \mathbb{V} + (\boldsymbol{\varphi}, \boldsymbol{\varphi}') \mathbb{V}^T \mathbb{R} \mathbb{V}. \quad (1.8)$$

Let $\boldsymbol{\varphi} = [\varphi_1, \varphi_2]^T$; hence, $\boldsymbol{\varphi}' = [\varphi_2, \varphi_1]^T$. Direct calculations and Lemma 1.1 give

$$(\boldsymbol{\varphi}, \boldsymbol{\varphi})^2 - (\boldsymbol{\varphi}, \boldsymbol{\varphi}')^2 = \varphi_1^4 + \varphi_2^4 + 2\varphi_1^2 \varphi_2^2 - 4\varphi_1^2 \varphi_2^2 = (\mathbb{D}\boldsymbol{\varphi}, \boldsymbol{\varphi})^2 = 1.$$

Therefore, there exists a number $z \in \mathfrak{R}^1$ such that $\|\boldsymbol{\varphi}\|^2 = \cosh(z)$ and $(\boldsymbol{\varphi}, \boldsymbol{\varphi}') = \sinh(z)$. Inserting this into (1.8), we obtain

$$\tilde{\mathbb{V}}^T \tilde{\mathbb{V}} = \cosh(z) \mathbb{V}^T \mathbb{V} + \sinh(z) \mathbb{V}^T \mathbb{R} \mathbb{V}. \quad (1.9)$$

Combining estimates (1.1) and (1.5) with representation (1.9), we obtain a one-dimensional minimization problem: Find $z_o \in \mathfrak{R}^1$ such that

$$z_o = \arg \inf_{\tilde{z} \in \mathfrak{R}^1} \left(\mu \cosh(\tilde{z}) + \lambda \sinh(\tilde{z}) \right) \quad (1.10)$$

where μ and λ are defined by (1.7).

Let $\mathbb{V}\mathbf{e}_k = [v_{1k}, v_{2k}]^T$. Note that this is a non-zero vector. Then, we have

$$\begin{aligned} \mu + \lambda &= \sum_{k=1}^3 \left((\mathbb{V}\mathbf{e}_k, \mathbb{V}\mathbf{e}_k) + (\mathbb{R}\mathbb{V}\mathbf{e}_k, \mathbb{V}\mathbf{e}_k) \right) = \sum_{k=1}^3 \left(v_{1k}^2 + v_{2k}^2 + 2v_{1k}v_{2k} \right) \\ &= \sum_{k=1}^3 (v_{1k} + v_{2k})^2 > 0 \end{aligned}$$

and

$$\mu - \lambda = \sum_{k=1}^3 (v_{1k} - v_{2k})^2 > 0.$$

We note that $\mu - \lambda \neq 0$, since the equality would imply that $v_{1k} = v_{2k}$, $k = 1, 2, 3$. In this case, the vectors $\mathbf{e}_1, \mathbf{e}_2, \mathbf{e}_3$ are collinear, which is possible only for a degenerate triangle.

Minimization problem (1.10) has the explicit solution:

$$z_o = \frac{1}{2} \ln \frac{\mu - \lambda}{\mu + \lambda}.$$

The number z_o corresponds to the matrix \mathbb{V}_o producing the metric

$$\mathfrak{M}_o \equiv \mathbb{V}_o^T \mathbb{V}_o = \frac{1}{\sqrt{\mu^2 - \lambda^2}} (\mu \mathbb{V}^T \mathbb{V} - \lambda \mathbb{V}^T \mathbb{R} \mathbb{V}) = \frac{1}{\sqrt{\mu^2 - \lambda^2}} \mathbb{V}^T \begin{bmatrix} \mu & -\lambda \\ -\lambda & \mu \end{bmatrix} \mathbb{V}.$$

This proves the theorem.

Note that the metric \mathfrak{M}_O differs from the metric

$$\mathfrak{M}_V = |\mathbb{H}_2| = \mathbb{V}^T \mathbb{V} \quad (1.11)$$

when $\lambda \neq 0$, although

$$\det \mathfrak{M}_V = \det \mathfrak{M}_O. \quad (1.12)$$

Thus, we have derived two independent metrics \mathfrak{M}_V and \mathfrak{M}_O yielding bounds (1.4) and (1.5), respectively. The proof of the theorem implies that there exist many metrics $\tilde{\mathbb{V}}^T \tilde{\mathbb{V}}$ produced by various values of z in formula (1.9). Hereafter, we use generational notation \mathfrak{M}_Δ to indicate any of these metrics, including the special metric \mathfrak{M}_O .

Combining (1.1) and (1.5), we get an upper bound on the interpolation error:

$$\|e_2\|_{L^\infty(\Delta)} \leq \frac{1}{8} \|\partial \Delta\|_{\mathfrak{M}_\Delta}^2 \quad (1.13)$$

where

$$\|\partial \Delta\|_{\mathfrak{M}_\Delta}^2 = \sum_{k=1}^3 \|\mathbf{e}_k\|_{\mathfrak{M}_\Delta}^2, \quad \|\mathbf{e}_k\|_{\mathfrak{M}_\Delta}^2 = (\mathfrak{M}_\Delta \mathbf{e}_k, \mathbf{e}_k).$$

Thus, the upper bound for the interpolation error includes the geometric quantities, i.e., the edge lengths $\|\mathbf{e}_k\|_{\mathfrak{M}_\Delta}$ measured in the constant tensor metric \mathfrak{M}_Δ . The lower bound for the interpolation error can be also expressed as a combination of geometric quantities associated with the triangle Δ . Let $\hat{\Delta}$ be the image of triangle Δ under the coordinate transformation $\hat{\mathbf{x}} = \mathbb{V} \mathbf{x}$. The estimate

$$\|e_2\|_{L^\infty(\Delta)} \geq \max_{k=1,2,3} \max_{\mathbf{x} \in \mathbf{e}_k} |e_2(\mathbf{x})| = \frac{1}{8} \max_{k=1,2,3} |(\mathbb{H}_2 \mathbf{e}_k, \mathbf{e}_k)| \geq \frac{1}{2\sqrt{5}} |\hat{\Delta}|$$

follows from the analysis presented in [11]. Note that

$$|\hat{\Delta}| = |\Delta| \det(\mathbb{V}) = |\Delta| \sqrt{\det(\mathbb{V}^T \mathbb{V})} = |\Delta| \sqrt{\det(\mathfrak{M}_\Delta)} = |\Delta|_{\mathfrak{M}_\Delta} \quad (1.14)$$

where $|\Delta|$ is the area of Δ and $|\Delta|_{\mathfrak{M}_\Delta}$ is its area in metric \mathfrak{M}_Δ . Thus, we have immediately that

$$\|e_2\|_{L^\infty(\Delta)} \geq \frac{1}{2\sqrt{5}} |\Delta|_{\mathfrak{M}_\Delta}. \quad (1.15)$$

Estimates (1.13) and (1.15) imply that the interpolation error $\|e_2\|_{L^\infty(\Delta)}$ is controlled from above and below by geometric quantities associated with the triangle Δ . We have proved the following result.

Theorem 1.2. Let u_2 be a quadratic function with a nonsingular Hessian $\mathbb{H}_2 = \mathbb{V}^T \mathbb{D} \mathbb{V}$ and e_2 denote its linear interpolation error on the triangle Δ . Let $\mathfrak{M}_\Delta = \mathbb{V}^T \mathbb{V}$. Then,

$$\frac{1}{2\sqrt{5}} |\Delta|_{\mathfrak{M}_\Delta} \leq \|e_2\|_{L^\infty(\Delta)} \leq \frac{1}{8} \|\partial \Delta\|_{\mathfrak{M}_\Delta}^2. \quad (1.16)$$

If $\det(\mathbb{H}_2) < 0$, the specific metric \mathfrak{M}_O provides the best upper bound in (1.16). The lower bound is the same for any metric \mathfrak{M}_Δ , since $|\Delta|_{\mathfrak{M}_\Delta}$ does not depend on the metric due to (1.14).

1.2. Illustrative example

In order to illustrate the diversity of metrics generated by (1.9), we consider the bilinear function $u_2 = xy$ with the indefinite Hessian

$$\mathbb{H}_2 = \begin{bmatrix} 0 & 1 \\ 1 & 0 \end{bmatrix}.$$

It is shown in [11] that for a quadratic function with an indefinite Hessian, the interpolation error achieves its maximum on the boundary of the triangle Δ :

$$\|e_2\|_{L^\infty(\Delta)} = \frac{1}{8} \max_{k=1,2,3} |(\mathbb{H}_2 \mathbf{e}_k, \mathbf{e}_k)|.$$

Let us apply this result to various meshes with a characteristic mesh size h schematically shown in Fig. 1. Consider a triangle Δ_1 from the isotropic mesh, e.g. the one with vertices $\mathbf{v}_1 = [0, 0]^T$, $\mathbf{v}_2 = [h, h]^T$, and $\mathbf{v}_3 = [0, h]^T$. The interpolation error on this triangle is

$$\|e_2\|_{L^\infty(\Delta_1)} = |(\mathbb{H}_2 \mathbf{e}_3, \mathbf{e}_3)| = \frac{1}{4} h^2 = \frac{1}{2} |\Delta_1|.$$

Due to the mesh structure, the interpolation error is the same for all triangles.

Consider a triangle Δ_2 from the first anisotropic mesh, e.g. the one with vertices $\mathbf{v}_1 = [0, 0]^T$, $\mathbf{v}_2 = [h, 1]^T$, and $\mathbf{v}_3 = [0, 1]^T$. The interpolation error on this triangle is

$$\|e_2\|_{L^\infty(\Delta_2)} = |(\mathbb{H}_2 \mathbf{e}_3, \mathbf{e}_3)| = \frac{1}{4} h = \frac{1}{2} |\Delta_2|.$$

Again, the interpolation error is the same for all triangles in this mesh. Exactly the same interpolation error holds true for the triangles in the second anisotropic mesh, e.g., for triangle Δ_3 with vertices $\mathbf{v}_1 = [0, 0]^T$, $\mathbf{v}_2 = [1, 0]^T$, and $\mathbf{v}_3 = [1, h]^T$.

Let all three meshes cover the unit square and have the same number of triangles, N . Then, the interpolation error equals to $1/(2N)$ in all three examples. These three meshes represent three different families of meshes yielding the optimal (i.e. reciprocal to N) reduction of the interpolation error. Thus, these meshes belong to three different families of quasi-optimal meshes. One family contains shape-regular

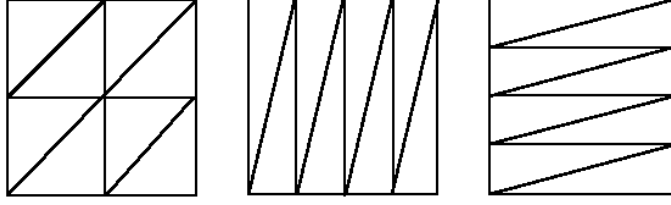


Figure 1. Illustration of one isotropic and two anisotropic meshes.

meshes; while the other two contain anisotropic meshes stretched in x and y directions, respectively.

Consider the following decomposition of Hessian \mathbb{H}_2 :

$$\mathbb{H}_2 = \mathbb{V}^T \begin{bmatrix} 1 & 0 \\ 0 & -1 \end{bmatrix} \mathbb{V}, \quad \mathbb{V} = \frac{1}{\sqrt{2}} \begin{bmatrix} 1 & 1 \\ 1 & -1 \end{bmatrix}.$$

Using formula (1.11), we obtain the isotropic metric $\mathfrak{M}_V = |\mathbb{H}_2| = \mathbb{I}$. Only triangles from isotropic meshes are shape-regular in metric \mathfrak{M}_V . However, using formulas (1.6)-(1.7), we obtain

$$\mathfrak{M}_O(\Delta_1) = \begin{bmatrix} 1 & 0 \\ 0 & 1 \end{bmatrix}, \quad \mathfrak{M}_O(\Delta_2) = \begin{bmatrix} h^{-1} & 0 \\ 0 & h \end{bmatrix}, \quad \mathfrak{M}_O(\Delta_3) = \begin{bmatrix} h & 0 \\ 0 & h^{-1} \end{bmatrix}.$$

Note that the triangles Δ_k are shape-regular in the respective metrics $\mathfrak{M}_O(\Delta_k)$, $k = 1, 2, 3$.

1.3. Bounds for C^2 -functions

Let u be a continuous function and $\mathcal{I}_{2,\Delta}(u)$ be its quadratic Lagrange interpolant on the triangle Δ . In Theorem 1.2, we have derived the geometric representation of the L^∞ -norm of $e_{2,\Delta} = \mathcal{I}_{2,\Delta}(u) - \mathcal{I}_{1,\Delta}(u)$. It was shown in [2] that the norm of $e_{2,\Delta}$ provides a good approximation for the corresponding norm of the true error $e_\Delta = u - \mathcal{I}_{1,\Delta}(u)$. For completeness, we formulate this result in the next lemma. Let \mathcal{F} be a space of symmetric 2×2 matrices. We define the following quantity:

$$\|\partial\Delta\|_{|\mathbb{H}|}^2 = \sum_{k=1}^3 \|\mathbf{e}_k\|_{|\mathbb{H}|}^2, \quad \|\mathbf{e}_k\|_{|\mathbb{H}|}^2 = \max_{\mathbf{x} \in \Delta} (|\mathbb{H}(\mathbf{x})| \mathbf{e}_k, \mathbf{e}_k). \quad (1.17)$$

Lemma 1.2 [2]. *Let $u \in C^2(\bar{\Delta})$. Then*

$$\frac{3}{4} \|e_{2,\Delta}\|_{L^\infty(\Delta)} \leq \|e_\Delta\|_{L^\infty(\Delta)} \leq \|e_{2,\Delta}\|_{L^\infty(\Delta)} + \frac{1}{4} \inf_{\mathbb{F} \in \mathcal{F}} \|\partial\Delta\|_{|\mathbb{H}-\mathbb{F}|}^2. \quad (1.18)$$

The second term in the right inequality is typical for contemporary *a posteriori* error analysis. It depends on the triangle and the particular features of the function u . In many cases it is essentially smaller than $\|e_{2,\Delta}\|_{L^\infty(\Delta)}$. An example will be considered at the end of this section.

Local analysis is naturally extended to triangulations. Let \mathfrak{M} be a piecewise constant metric composed of local metrics \mathfrak{M}_Δ . Let $N(\Omega_h)$ be the number of triangles in the mesh Ω_h . If Ω_h is a quasi-uniform mesh with respect to metric \mathfrak{M} , then all triangles have approximately the same area measured in this metric:

$$N(\Omega_h)^{-1}|\Omega|_{\mathfrak{M}} \simeq |\Delta|_{\mathfrak{M}_\Delta} \simeq |\partial\Delta|_{\mathfrak{M}_\Delta}^2 \quad \forall \Delta \in \Omega_h$$

where $a \simeq b$ means the existence of a constant C independent of the mesh and the triangle such that $C^{-1}a \leq b \leq Ca$. Hereafter, C denotes a generic constant. Thus, the following error estimate is obtained

$$\|e\|_{L^\infty(\Omega)} = \max_{\Delta \in \Omega_h} \|e\|_{L^\infty(\Delta)} \leq C \max_{\Delta \in \Omega_h} |\Delta|_{\mathfrak{M}_\Delta} \leq C |\Omega|_{\mathfrak{M}} N(\Omega_h)^{-1} \quad (1.19)$$

which implies the asymptotically optimal error reduction and proves the quasi-optimality of \mathfrak{M} -quasi-uniform meshes. We note that different metrics \mathfrak{M} produce the same area $|\Omega|_{\mathfrak{M}}$, since the triangle areas are the same due to (1.14). Therefore, error estimate (1.19) should be close for the meshes from different families with the same number of elements $N(\Omega_h)$.

Let us return to Lemma 1.2 and consider, for instance, a quasi-optimal mesh Ω_h generated by $\mathfrak{M}_\Delta = \mathfrak{M}_V = |\mathbb{H}_2|$ and characterized by the balance between the volume and the perimeter of its triangles:

$$|\Delta|_{\mathfrak{M}_\Delta} \simeq \|\partial\Delta\|_{\mathfrak{M}_\Delta}^2 \quad \forall \Delta \in \Omega_h.$$

Using (1.15) and the fact that \mathbb{H}_2 is a constant Hessian of $\mathcal{S}_{2,\Delta}(u)$, we obtain

$$\|e_{2,\Delta}\|_{L^\infty(\Delta)} \geq C^{-1} \|\partial\Delta\|_{\mathfrak{M}_\Delta}^2 = C^{-1} \|\|\partial\Delta\|\|_{\mathfrak{M}_\Delta}^2.$$

Therefore, for a function with a nonsingular Hessian, we obtain

$$\frac{\inf_{\mathbb{F} \in \mathcal{F}} \|\|\partial\Delta\|\|_{|\mathbb{H}-\mathbb{F}|}^2}{\|e_{2,\Delta}\|_{L^\infty(\Delta)}} \leq C \frac{\inf_{\mathbb{F} \in \mathcal{F}} \|\|\partial\Delta\|\|_{|\mathbb{H}-\mathbb{F}|}^2}{\|\|\partial\Delta\|\|_{\mathfrak{M}_\Delta}^2} = C \frac{\inf_{\mathbb{F} \in \mathcal{F}} \|\|\partial\Delta\|\|_{|\mathbb{H}-\mathbb{F}|}^2}{\|\|\partial\Delta\|\|_{|\mathbb{H}_2|}^2} = o(1).$$

This argument justifies the use of the quadratic Lagrange interpolant for the derivation of the optimal metric for functions $u \in C^2(\Delta)$ with nonsingular Hessians on quasi-optimal meshes.

2. Numerical experiments

Generation of a quasi-optimal mesh for a given function u is in general an iterative process. First, we generate an initial mesh with a desirable number of elements and calculate a piecewise constant metric \mathfrak{M} . Second, we generate a new

mesh, which is quasi-uniform in metric \mathfrak{M} . Also, we require that the number of triangles in the new mesh is approximately the same as in the initial mesh. To generate a \mathfrak{M} -quasi-uniform mesh, we use a sequence of local mesh modifications described in [18] and implemented in the publicly available package Ani2D (<http://sourceforge.net/projects/ani2d>). Frequently, the initial mesh is not related to the function u , which results in a large interpolation error and a non-optimal metric \mathfrak{M} . In this case, the two-step adaptation process can be repeated (see Algorithm 2.1). A few iterations may be required until the interpolation error is stabilized. The number of iterations depends on the smoothness of the function u .

Algorithm 2.1. Adaptive mesh generation

- 1: Generate an initial mesh Ω_h and compute the metric \mathfrak{M} .
 - 2: **loop**
 - 3: Generate a \mathfrak{M} -quasi-uniform mesh Ω_h with the prescribed number of triangles.
 - 4: Recompute the metric \mathfrak{M} .
 - 5: If Ω_h is \mathfrak{M} -quasi-uniform, then exit the loop
 - 6: **end loop**
-

In practice, Algorithm 2.1 converges faster and results in a smoother mesh when the metric is continuous. To define a continuous metric we use the method of shifts. For every node \mathbf{v}_i in Ω_h , we define the superelement σ_i as the union of all triangles sharing \mathbf{v}_i . Then, $\mathfrak{M}(\mathbf{v}_i)$ is defined as one of the metrics in σ_i with the largest determinant. This method always chooses the worst metric in the superelement. Once the metric is computed at the nodes of each triangle, it is linearly interpolated inside the triangles.

We consider three examples of functions with indefinite Hessians. Their isolines are presented in Fig.2. In the experiments we study the asymptotic behaviour of the P_1 interpolation error for two families of quasi-optimal meshes based on the local metrics $\mathfrak{M}_V = \mathbb{V}^T \mathbb{V}$ and $\mathfrak{M}_O = \mathbb{V}_o^T \mathbb{V}_o$, respectively. The matrix \mathbb{V} was calculated using the LAPACK routine DSYEV that computes eigenvalues and eigenvectors of a real symmetric matrix.

Let Ω be the unit square in all examples. The first function is the canonical hyperbolic function,

$$u^{(1)}(x, y) = (x - 0.5)^2 - (y - 0.5)^2,$$

with the constant indefinite Hessian $\mathbb{H}_2 = \text{diag}\{2, -2\}$. The isolines of this function are shown in the left pattern in Fig. 2. Figure 3 shows the first two meshes in two sequences of quasi-optimal meshes with approximately 4000 and 8000 triangles. The meshes in the top row are quasi-uniform in the metric \mathfrak{M} generated by local metrics \mathfrak{M}_O . The meshes in the bottom row are quasi-uniform in the metric \mathfrak{M} generated by local metrics \mathfrak{M}_V . Obviously both sequences are different, one contains strongly anisotropic meshes stretched along the bisectors of four quadrants, while the other one contains isotropic meshes. The data in Table 1 also confirm that. The second and the fifth columns in this table show the maximal ratio of the circumscribed radius

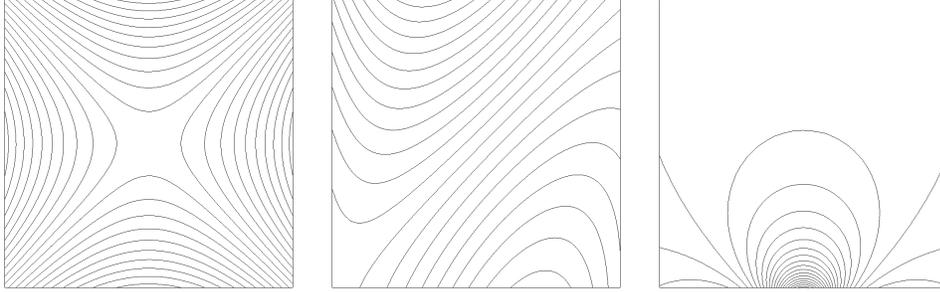


Figure 2. From left to right: isolines of functions $u^{(1)}$, $u^{(2)}$, and $u^{(3)}$.

Table 1.
Example 1. Interpolation error for two families of quasi-optimal meshes.

$\mathfrak{M}_\Delta = \mathfrak{M}_O$			$\mathfrak{M}_\Delta = \mathfrak{M}_V$		
$N(\Omega_h)$	R/r	$\ e_h\ _{L^\infty(\Omega)}$	$N(\Omega_h)$	R/r	$\ e_h\ _{L^\infty(\Omega)}$
4073	834.2	7.974e-05	3930	15.1	8.195e-05
8267	768.1	4.054e-05	7885	24.6	4.064e-05
16589	1121.	2.047e-05	15813	18.7	2.040e-05
33118	2259.	1.053e-05	31786	27.9	1.018e-05
66557	4794.	5.233e-06	63373	46.2	5.126e-06
rate		0.991			0.936

R to the inscribed radius r across all triangles in the mesh. The interpolation errors are proportional to $N(\Omega_h)^{-1}$, which is the optimal error reduction. Thus, both sequences contain quasi-optimal meshes. Moreover, the errors in two sequences differ by 1–3% only.

The second function is

$$u^{(2)}(x,y) = (x + \sin(\pi x))^2 - (y + \sin(\pi x))^2.$$

The isolines of this function are shown in the middle pattern in Fig. 2. The Hessian of this function is indefinite almost everywhere in the computational domain except for a parabola-shaped region around point $(0.6, 0.4)$. This region can be identified in the top-right pattern in Fig. 4 as the region where the mesh is isotropic. Each row in this figure shows two meshes with approximately 4000 and 8000 triangles. The top and bottom rows correspond to local metrics \mathfrak{M}_O and \mathfrak{M}_V , respectively. Clearly, metric (1.6) results in more stretched meshes.

The interpolation errors presented in Table 2 verify that both metrics result in quasi-optimal meshes. The error decrease is again proportional to $N(\Omega_h)^{-1}$, i.e. both sequences contain quasi-optimal meshes. The values of the maximal anisotropy ratio, R/r , confirm the visual impression that one sequence of meshes is much more

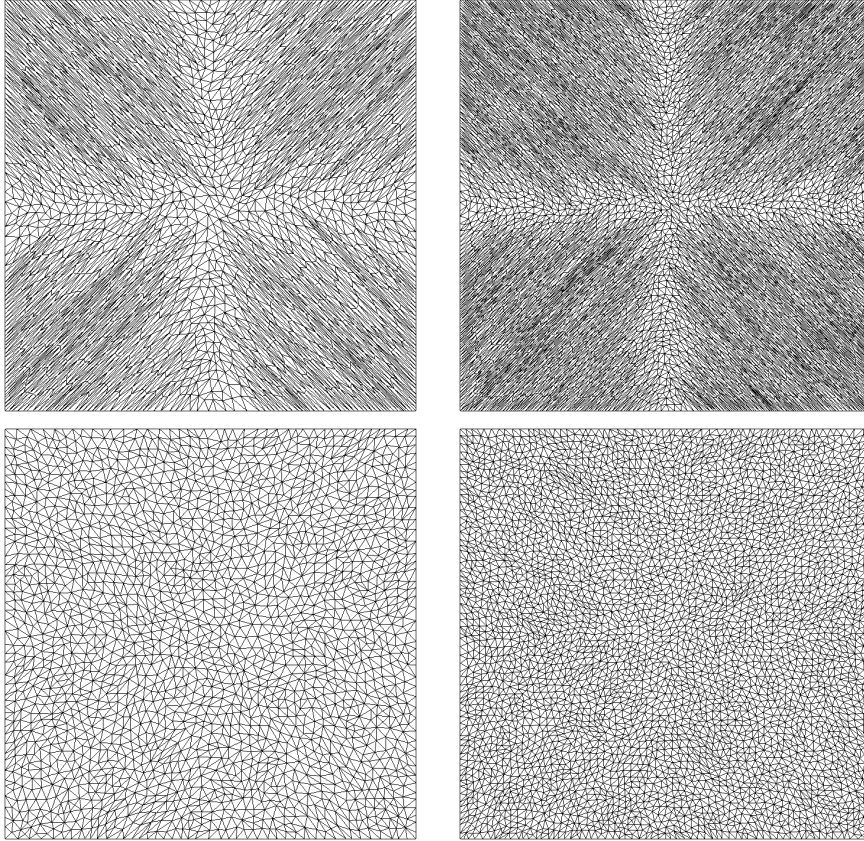


Figure 3. Example 1. Quasi-optimal meshes with approximately 4000 (left column) and 8000 (right column) triangles. The top and bottom rows correspond to two different families of meshes.

Table 2.

Example 2. Interpolation error for two families of quasi-optimal meshes.

$\mathfrak{M}_\Delta = \mathfrak{M}_O$			$\mathfrak{M}_\Delta = \mathfrak{M}_V$		
$N(\Omega_h)$	R/r	$\ e_h\ _{L^\infty(\Omega)}$	$N(\Omega_h)$	R/r	$\ e_h\ _{L^\infty(\Omega)}$
4070	2489.	9.523e-04	3934	62.0	8.818e-04
8097	1492.	5.393e-04	7839	82.6	3.977e-04
16269	937.1	2.281e-04	15761	203.	2.376e-04
32881	2704.	1.209e-04	31478	190.	1.374e-04
65147	4142.	6.427e-05	63031	239.	5.837e-05
rate		0.991			0.936

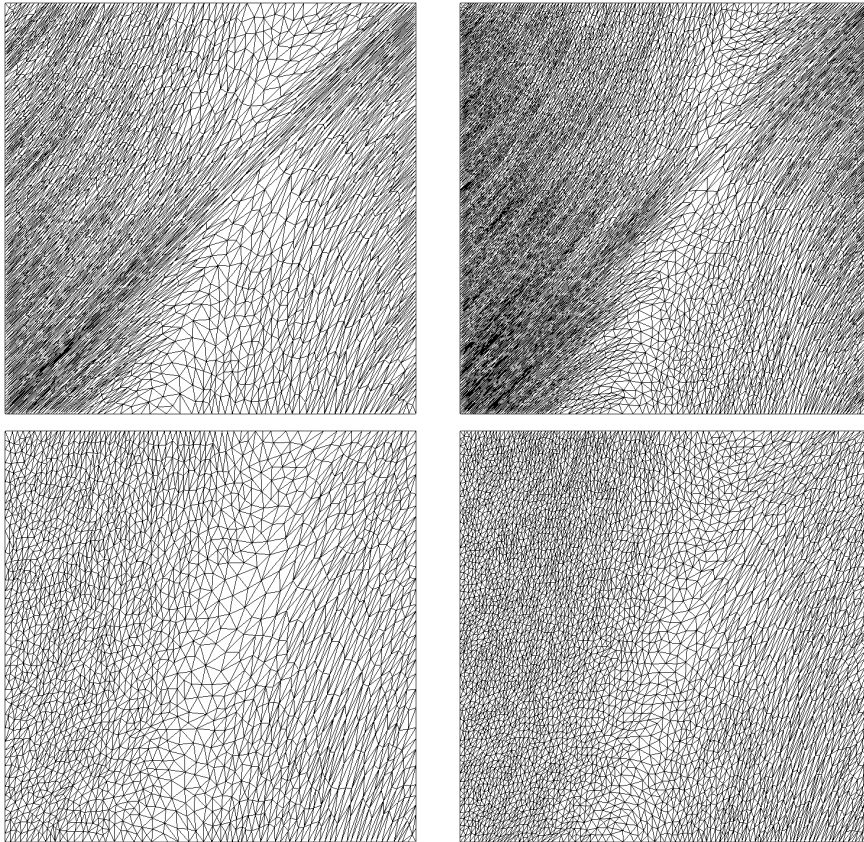


Figure 4. Example 2. Quasi-optimal meshes with approximately 4000 (left column) and 8000 (right column) triangles. The top and bottom rows correspond to two different families of meshes.

Table 3.

Example 3. Interpolation error for two families of quasi-optimal meshes.

$\mathfrak{M}_\Delta = \mathfrak{M}_O$			$\mathfrak{M}_\Delta = \mathfrak{M}_V$		
$N(\Omega_h)$	R/r	$\ e_h\ _{L^\infty(\Omega)}$	$N(\Omega_h)$	R/r	$\ e_h\ _{L^\infty(\Omega)}$
4003	380.1	2.643e-03	3946	19.0	2.562e-03
8087	353.2	1.285e-03	7872	12.8	1.295e-03
16069	652.0	6.502e-04	15776	10.9	6.457e-04
32206	955.7	3.283e-04	31579	11.8	3.254e-04
64478	5291.	1.647e-04	62970	26.3	1.620e-04
rate		0.996	rate		0.996

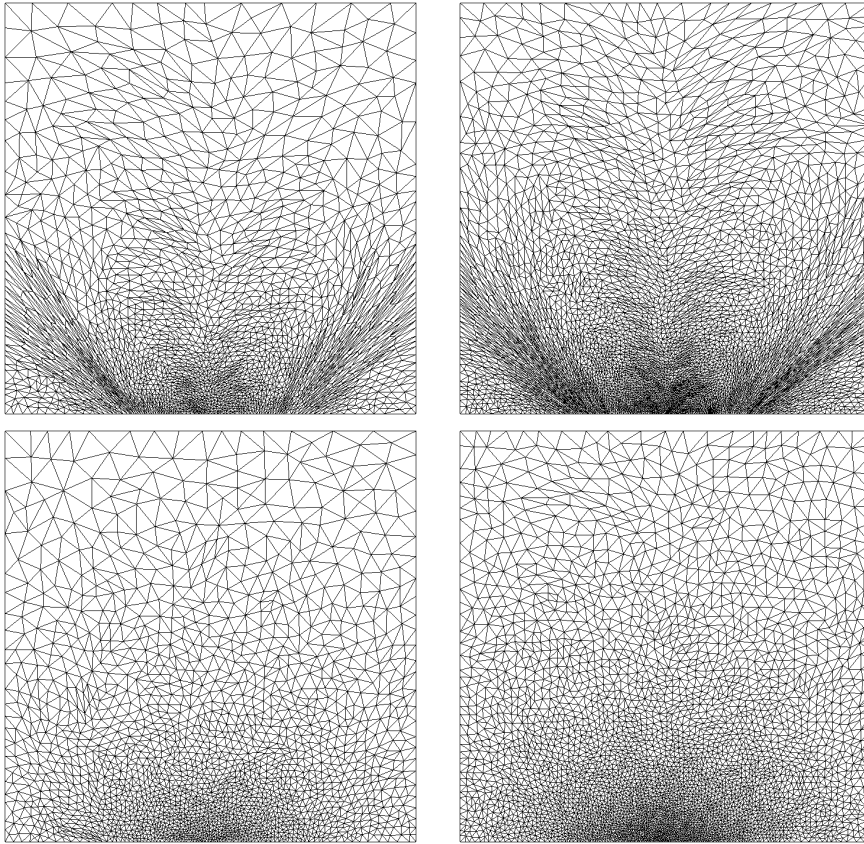


Figure 5. Example 3. Quasi-optimal meshes with approximately 4000 (left column) and 8000 (right column) triangles. The top and bottom rows correspond to two different families of meshes.

stretched than the other. Thus, for this example there exist at least two different families of quasi-optimal meshes. There is no conclusive evidence that one sequence of meshes gives a consistently smaller error.

The third function

$$u^{(3)}(x, y) = \frac{(x - 0.5)^2 - (y + 0.2)^2}{((x - 0.5)^2 + (y + 0.2)^2)^2}$$

satisfies the Laplace equation. Its isolines are shown in the right pattern in Fig. 2. Figure 5 is identical to Figs. 3 and 4. The top and bottom rows present the two first meshes in different sequences of quasi-optimal meshes. One observes the presence of two anisotropic jet-like structures in the top pattern.

The interpolation errors presented in Table 3 verify that both metrics result in quasi-optimal meshes. The errors are again proportional to $N(\Omega_h)^{-1}$, which is the

optimal error reduction. As in the first example, they are within 1-3% of one another, which indicates that neither of the sequences is preferable for minimizing the interpolation error.

3. Conclusion

We have extended the theory of optimal meshes that minimize the P_1 interpolation error for a given function u . When the Hessian of u is indefinite, we have shown that there exists a family of quasi-optimal meshes that give approximately the same interpolation error, contain the same number of triangles, but have drastically different properties. One mesh can be isotropic, while the other one is anisotropic. These quasi-optimal meshes are generated by different metric fields. Formally, one of the metrics can be referred to as an optimal one, since it provides the sharpest bounds for the local interpolation error. In future, we shall analyze the behaviour of the discretization error for a family of quasi-optimal meshes.

The existing metric-based mesh generation technology is capable of producing any quasi-optimal mesh in a family. The result depends on the initial mesh selected for adaptive iterations. In future, we shall analyze this phenomenon in more detail.

References

1. A. Agouzal, K. Lipnikov, and Y. Vassilevski, Adaptive generation of quasi-optimal tetrahedral meshes. *East-West J. Numer. Math.* (1999) **7**, 223–244.
2. A. Agouzal, K. Lipnikov, and Y. Vassilevski, Hessian-free metric-based mesh adaptation via geometry of interpolation error. *Comp. Math. Math. Phys.* (2010) **50**, 124–138.
3. A. Agouzal and Y. Vassilevski, Minimization of gradient errors of piecewise linear interpolation on simplicial meshes. *Comp. Meth. Appl. Mech. Engrg.* (2010) **199**, 2195–2203.
4. A. Agouzal, K. Lipnikov, and Y. Vassilevski, Edge-based *a posteriori* error estimators for generating quasi-optimal simplicial meshes. *Math. Model. Nat. Phenom.* (2010) **5**, 91–96.
5. A. Agouzal, K. Lipnikov, and Y. Vassilevski, On optimal convergence rate of finite element solutions of boundary value problems on adaptive anisotropic meshes. *Math. Comp. Simul.* (2011) **81**, No. 10, 1949–1961.
6. H. Borouchaki, F. Hecht, P. J. Frey, Mesh gradation control, *Int. J. Numer. Meth. Engrg.* (1998) **43**, 1143–1165.
7. G.C. Buscaglia, D.A. Dari. Anisotropic mesh optimization and its application in adaptivity. *Int. J. Numer. Meth. Engrg.* (1997) **40**, 4119–4136.
8. L. Chen, P. Sun, and J. Xu, Optimal anisotropic meshes for minimizing interpolation errors in L^p -norm. *Math. Comp.* (2007) **76**, 179–204.
9. P. G. Ciarlet, *The Finite Element Method for Elliptic Problems*. North-Holland, 1978.
10. T. Coupez, Generation de maillage et adaptation de maillage par optimisation locale. *Revue Européenne des Elements Finis* (2000) **49**, 403–423.
11. E. D’Azevedo, Optimal triangular mesh generation by coordinate transformation. *SIAM J. Sci. Stat. Comp.* (1991) **12**, 755–786.

12. P. E. Farrell and J. R. Maddison, Conservative interpolation between volume meshes by local Galerkin projection, *Comp. Meth. Appl. Mech. Engrg.* (2011) **200**, 89–100.
13. M. Fortin, M.-G. Vallet, J. Dompierre, Y. Bourgault, and W. G. Habashi, *Anisotropic mesh adaptation: theory, validation and applications Computational Fluid dynamics*. John Wiley & Sons Ltd., 1996.
14. P. L. George, *Automatic mesh generation: Applications to Finite Element Methods*. John Wiley & Sons, New York, 1991.
15. W. Huang and W. Sun, Variational mesh adaptation II: Error estimates and monitor functions. *J. Comp. Phys.* (2003) **184**, 619–648.
16. W. Huang, Metric tensors for anisotropic mesh generation. *J. Comp. Phys.* (2005) **204**, 633–665.
17. A. Loseille and F. Alauzet, Optimal 3D highly anisotropic mesh adaptation based on the continuous mesh framework. In: *Proc. of 18th Int. Meshing Roundtable* (Ed. B. W. Clark). (2009) 575–594.
18. Y. Vassilevski and K. Lipnikov, Adaptive algorithm for generation of quasi-optimal meshes. *Comp. Math. Math. Phys.* (1999) **39**, 1532–1551.
19. Y. Vassilevski and A. Agouzal, An unified asymptotic analysis of interpolation errors for optimal meshes. *Doklady Math.* (2005) **72**, 879–882.